Icarus 257 (2015) 217–220

Contents lists available at ScienceDirect

Icarus

journal homepage: www.elsevier.com/locate/icarus

Note

Hot CH_4 in the polar regions of Jupiter

Sang Joon Kim [a,*], Chae Kyung Sim [a], Jin Ho [a], Thomas R. Geballe [b], Yuk L. Yung [c], Steve Miller [d], Yong Ha Kim [e]

[a] School of Space Research, Kyung Hee University, Yongin 446-701, South Korea
[b] Gemini Observatory, 670 N. A'ohoku Place, Hilo, HI 96720, USA
[c] Division of Geological and Planetary Sciences, Caltech, Pasadena, CA 91125, USA
[d] Department of Physics and Astronomy, University College London, London WC1E 6BT, UK
[e] Department of Astronomy and Space Science, Chungnam National University, Daejeon 305-764, South Korea

ARTICLE INFO

Article history:
Received 19 January 2015
Revised 27 March 2015
Accepted 7 May 2015
Available online 15 May 2015

Keywords:
Jupiter
Spectroscopy
Aurorae
Infrared observations
Atmospheres, composition

ABSTRACT

We have obtained 3.3–3.4-μm spectro-images of Jupiter including CH_4 and H_3^+ emission lines from both polar regions at the Gemini North telescope. We find that the peak of the 3-μm CH_4 northern bright spot is located at ~200° (SysIII) longitude, ~20° west of the center of the 8-μm north-polar bright spot, and does not coincide with the 3-μm H_3^+ bright spot. We derive high temperatures (500–850 K) from CH_4 rotational lines on the bright spots of both polar regions, above the 1-μbar pressure level, while we find cooler temperatures (<350 K) over the 8-μm spot. The intensity ratios of the various 3-μm vibrational bands of CH_4 are roughly constant, indicating that the upper states of these bands are mostly populated by non-thermal excitation mechanisms, such as auroral particle precipitation and/or Joule heating, in contrast with the 8-μm thermal emission.

1. Introduction

The region of the 8-μm north-polar brightening of CH_4, which is known to be warmer than the surrounding polar region (Kim et al., 1985; Drossart et al., 1993), has been observed to be stationary at 180° (SysIII) longitude since the early 1980s (Caldwell et al., 1983; Sada et al., 2003; Greathouse, private communication, 2014), whereas the south-polar bright spot has been observed to wander between 268°W and 96°E (SysIII) longitude in the south polar region (Caldwell et al., 1988). The morphology of the northern 8-μm CH_4 bright spot is similar to that of the 13-μm C_2H_2 polar emission (Sada et al., 2003), but it is very different from that of the H_3^+ auroral oval (Satoh et al., 1996) suggesting a significantly different excitation process for the two hydrocarbons than for H_3^+.

The 3-μm polar (and presumably auroral) CH_4 emission was first reported in 1991 in ProtoCAM images of Jupiter (Kim et al., 1991) obtained at the NASA Infrared Telescope Facility. Nearly two decades later enhanced 3-μm CH_4 emission from a small area near the south pole was detected with CGS4 on the United Kingdom Infrared Telescope (UKIRT) (Kim et al., 2009). The interpretation of the 3-μm CGS4 CH_4 spectrum was hampered, however, by its low signal-to-noise (S/N) ratio. It was difficult to disentangle the ν_3, $\nu_3 + \nu_4 - \nu_4$, and $\nu_2 + \nu_3 - \nu_2$ lines of CH_4 from the complicated structure of the CH_4 bands, nor was it possible to compare the morphology of the 3-μm CH_4 emission with that of the 8-μm CH_4 polar brightening for the study of the excitation processes of these vibrational bands.

2. Observations and data reduction

In order to investigate the excitation processes of CH_4 in the auroral regions, we have obtained $R \sim 18{,}000$ spectra at significantly improved S/N ratio of the north and south polar regions in the 3.30–3.39 μm interval using the Gemini Near-Infrared Spectrograph (GNIRS) with a 0.1 arcsec wide slit, at Gemini North on January 13, and February 4, 2013 (UT), respectively. The relative velocities of Earth and Jupiter were 20.60 and 26.26 km/s, respectively, which allowed the partial separation of the lines of the fundamental ν_3 band of CH_4 from their telluric counterparts. The spectral region observed also contained lines of the $\nu_3 + \nu_4 - \nu_4$ and $\nu_2 + \nu_3 - \nu_2$ bands (Kim and Geballe, 2005; Kim et al., 2014), which do not have significant telluric counterparts, although some of them are obscured by other telluric absorption lines. We oriented the 0.1 arcsec wide slit perpendicular to the central meridian and stepped in latitude from just off of each pole through each polar region, using 0.8 arcsec steps with an exposure time of 4 min for each latitude. The atmospheric seeing at 3.3 μm was 0.5–0.6 arcsec; thus the raw data are undersampled in latitude and highly oversampled in longitude (the array pixel dimension was 0.0513 arcsec on the sky). In the longitudinal direction the data were binned by ~0.5 arcsec to match the latitudinal sampling more closely. Since even at the lowest latitudes Jupiter covered no more than 25 arcsec within the 49 arcsec slit, it was possible to nod the telescope along the slit and observe Jupiter 100% of the time, using the sky portions in the preceding or succeeding spectro-images to subtract the sky emission. The limb positions were determined by where the intensities from the disk decrease rapidly, but limb brightening or darkening produces an uncertainty of ~0.3 arcsec in the limb positions. Taking seeing into account we estimate the total uncertainty in the longitudinal direction to be less than 1 arcsec. However, the *relative* positions of the H_3^+ and CH_4 bright spots are accurate to much better than the seeing limit because they were measured on the same spectro-images.

* Corresponding author at: School of Space Research, Kyunghee University, Yongin, Kyunggido 446-701, South Korea.
E-mail address: sjkim1@khu.ac.kr (S.J. Kim).

http://dx.doi.org/10.1016/j.icarus.2015.05.008
0019-1035/

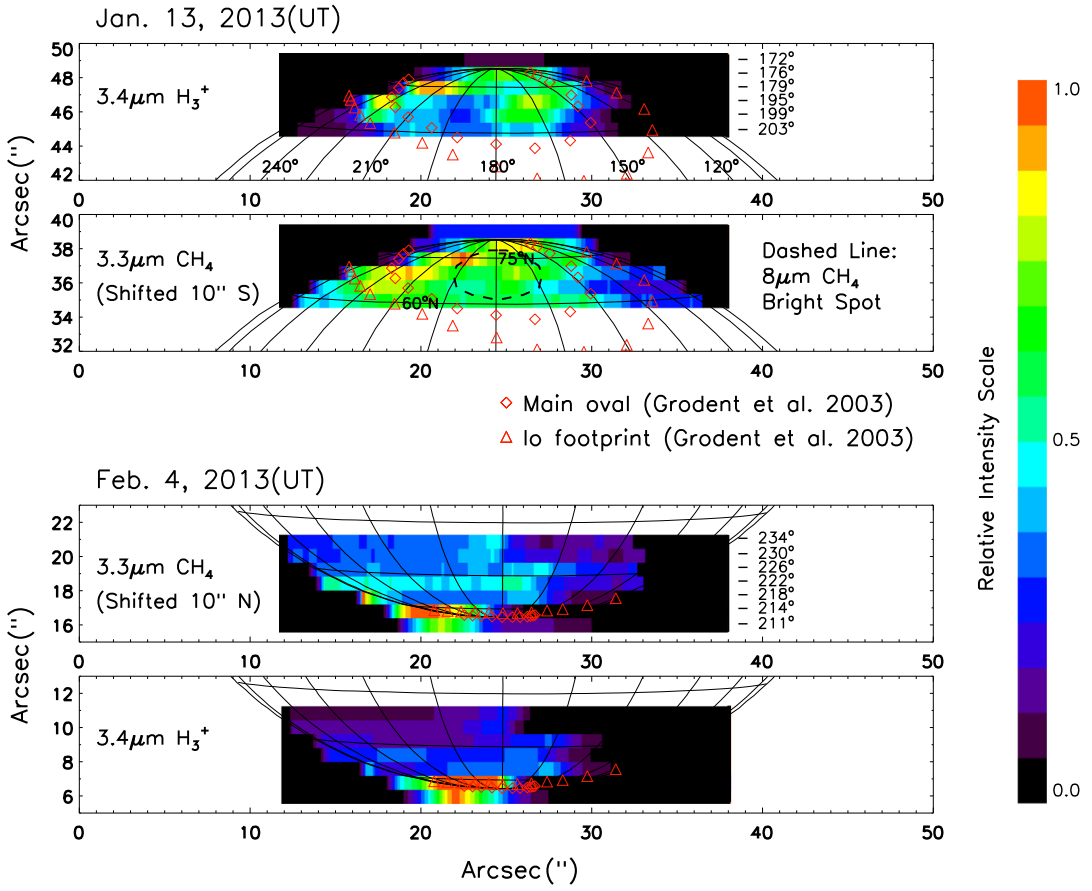

Fig. 1. 3-μm CH_4 and H_3^+ images of jovian polar regions extracted from their strong emission lines. Dates of the observations are as shown; and the north and south polar figure panels for the CH_4 emissions are shifted 10 arcsec southward and northward, respectively, for clear comparisons with the corresponding H_3^+ figure panels. The central meridian longitudes (CMLs) at the times of the observations are shown at right; in the assembled images the stripes have been coordinate-transformed so that CMLs are 180° (SysIII). The position of the north-polar bright emission by hydrocarbons is shown (e.g., http://photojournal.jpl.nasa.gov/catalog/PIA13699; Sada et al., 2003) as well as the boundaries of the Io footprints and the main ovals observed in the ultraviolet (Grodent et al., 2003; part of the boundary of the southern region is over or near the horizon). Dark areas are where data are not available or intensities are relatively very low. The H_3^+ and CH_4 emission intensities are normalized to the brightest regions in the images to produce a common color scale (shown at right). (For interpretation of the references to color in this figure legend, the reader is referred to the web version of this article.)

3. Morphology and temperatures

Fig. 1 contains 3.3-μm CH_4 and 3.4-μm H_3^+ images of Jupiter extracted from strong CH_4 and H_3^+ emission lines in the spectra. The CH_4 lines are shown in Fig. 2; a complex of strong 3.4-μm H_3^+ lines (not shown in Fig. 2; see Fig. 6 of Kim et al. (2010) for example), which do not overlap with strong CH_4 lines, are used to construct the H_3^+ images in Fig. 1. The latitudinal stripes observed at different times are shifted and are stretched or compressed so that the longitudes for each stripe align and the central meridian is 180° (SysIII). The CMLs at the times of the observations, and the Io footprints and the main ovals observed in the ultraviolet (Grodent et al., 2003) are shown. As can be seen, the brightest spot in the 3.3-μm CH_4 image of the north polar region, at longitude 200° and latitude 75°, is ~20° west of the center of the 8-μm CH_4 bright spot (thick dashed line). In addition, the overall shapes of the two bright regions differ significantly; the 3.3-μm bright region is more extended. The 3.3-μm CH_4 bright region also is not perfectly coincident with the H_3^+ bright spot, whose center is located at about longitude 215°. The southern CH_4 bright spot appears to be close to the H_3^+ bright spot, but the relative locations are not certain since most of the southern auroral CH_4 and H_3^+ emission occurs near or over the south polar horizon.

Fig. 2a and b shows spectra extracted from the northern and southern 3.3-μm bright regions. The wavelength ranges where ν_3, $\nu_3+\nu_4-\nu_4$, and $\nu_2+\nu_3-\nu_2$ lines dominate the emission from Jupiter, can be seen in the model spectra near the bottom of each panel. We derive temperatures from the rotational lines of the CH_4 bands using the following considerations. Radiative transfer programs that simulate the fluorescent emission of the 3-μm bands of CH_4 have been developed for analysis of jovian spectra (Drossart et al., 1999; Kim et al., 2009, 2010, 2014). For the CH_4 molecular line list, we adopt the HITRAN2012 database (Rothman et al., 2009). Since CH_4 is a spherical top molecule, its dipole moment is small, resulting in very low *rotational* Einstein A coefficients. For the rotational states we measured, the A coefficients are significantly less than collisional deexcitation rates in the auroral regions. Thus one may assume that the rotational-state populations of CH_4 are in LTE. The populations of excited vibrational states of CH_4 are probably not controlled by collisions, however, due to the high values of the *vibrational* Einstein A coefficients (Kim et al., 2014) compared to collision rates. Therefore, regardless of the energy sources (Wong et al., 2000, 2003) over the auroral regions, the rotational populations of the CH_4 states are governed by LTE, and the rotational structures of the CH_4 bands can be constructed by radiative transfer equations with Planckian source functions. The rotational temperatures derived from the intensities of individual lines of the various 3-μm bands of CH_4 thus reflect the local atmospheric temperatures.

In order to determine the nature of the vibrational band emission, we first constructed synthetic spectra at different rotational temperatures to be compared with the observations, and found the best-fit rotational temperatures of 500 ± 50 and 850 ± 70 K for the northern and southern bright spots, respectively, as presented in Fig. 2a and b. These temperatures are significantly higher than those derived from surrounding non-auroral zones and equatorial regions (Kim et al., 2014), and are even higher than the temperatures (<350 K) derived from the 3.3-μm spectra obtained at the location (160–200° (SysIII) longitude, and 60–80°N latitude) of the 8-μm bright spot (spectrum and fit not shown here).

We then examined the intensity ratios $\nu_3/\nu_3+\nu_4-\nu_4$, and $\nu_3/\nu_2+\nu_3-\nu_2$ as well as the intensities of these bands in order to determine whether the observed vibrational band emission from them is thermal or nonthermal. As seen in Fig. 3, the intensity ratios of the vibrational bands are relatively *constant* compared with the intensity profiles themselves in both polar regions. This is significant, because radiative excitation (by sunlight) of the ν_3 state and of the $\nu_3+\nu_4$ and $\nu_2+\nu_3$ states occurs at different wavelengths (3.3 μm and 2.3 μm, respectively). Since the spectrum of thermal radiation is determined by the blackbody temperature, it is not plausible that local thermal radiation can produce the observed uniform intensity ratios in the polar regions, where the temperatures, and hence the ratio of thermal radiation at 3.3 μm and 2.3 μm, vary drastically from

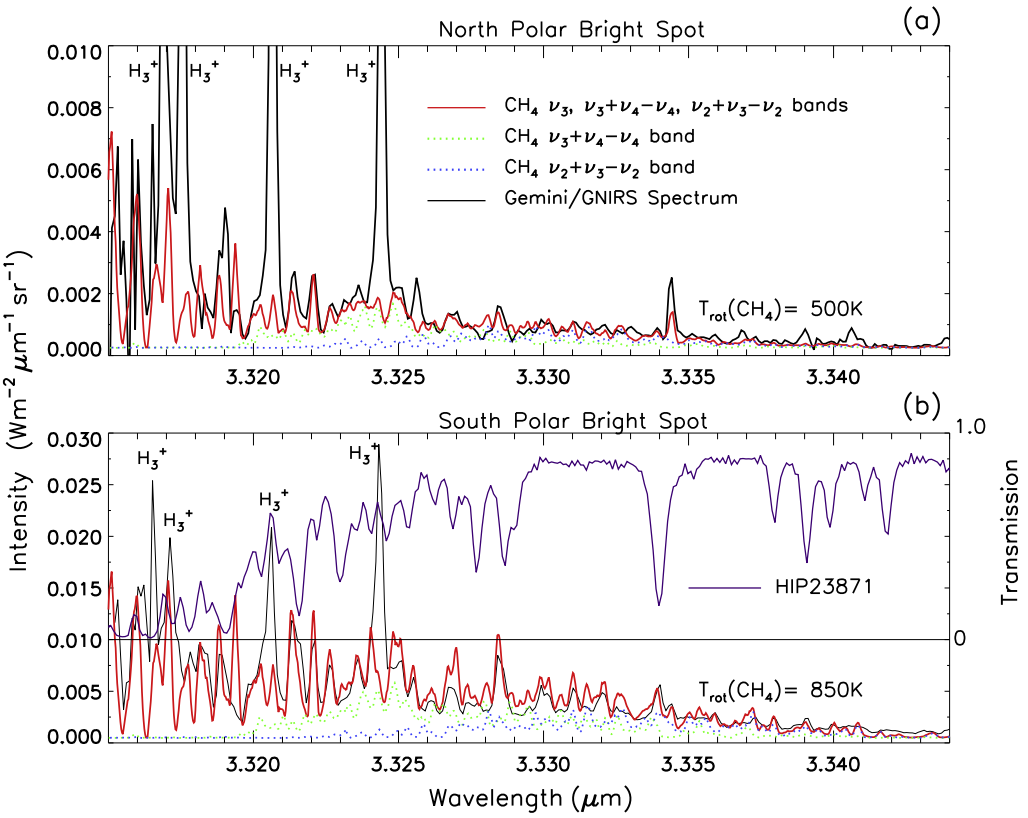

Fig. 2. (a) Comparison of the north polar bright spot with a CH_4 model spectrum with a 500 K rotational temperature (H_3^+ lines are not included in the model). The red line is the model sum of the contributions from all three CH_4 bands; the individual combination bands are shown as dots. The continuum levels in the spectra of the northern and southern bright spots are approximately 0.25 and 0.48 mW m^{-2} μm^{-1} sr^{-1}, respectively. The S/N ratio is ~3 for an intensity of 0.1 mW m^{-2} μm^{-1} sr^{-1}. (b) Comparison of the south polar bright spot with a CH_4 model spectrum with a 850 K rotational temperature. The spectrum of the standard star, HIP23871, used for correcting for telluric absorptions in the jovian spectra, is also shown. (For interpretation of the references to color in this figure legend, the reader is referred to the web version of this article.)

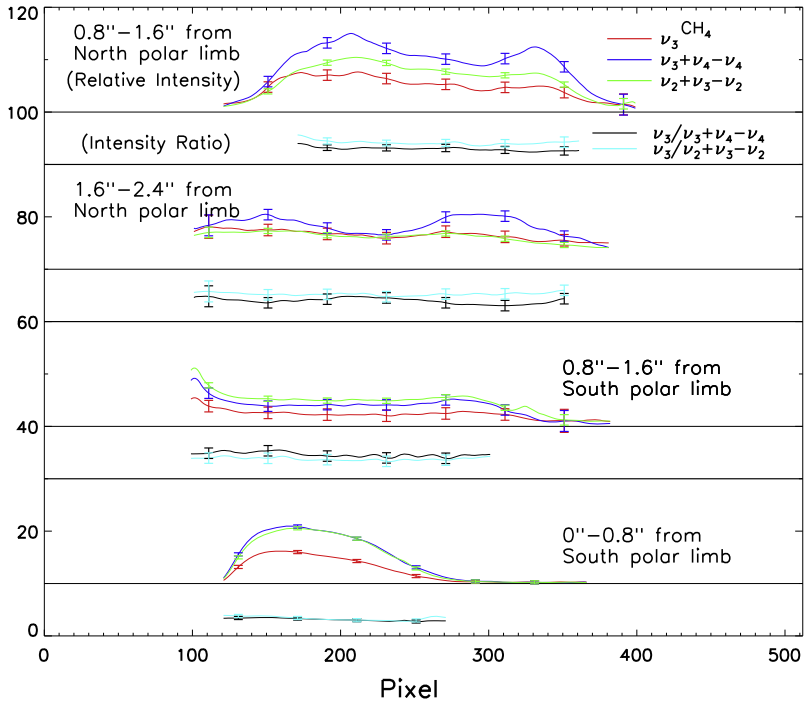

Fig. 3. The relative intensities of the ν_3 and $\nu_3+\nu_4-\nu_4$, $\nu_2+\nu_3-\nu_2$ bands of CH_4, and the intensity ratios $\nu_3/\nu_3+\nu_4-\nu_4$, and $\nu_3/\nu_2+\nu_3-\nu_2$ for the four stripes containing bright line emission, in each polar region. From the top of this figure, the approximate latitudinal ranges at the central meridian for the four stripes are 70–78°N, 66–70°N, 64–70°S, and 70–90°S. The intensity ratios near the limbs are uncertain due to low signals, and those data with large error bars were cut off. $1-\sigma$ error bars are shown. Note the relatively uniform intensity ratios in both polar regions, although the relative intensities vary with longitude.

region to region. A good example of a uniform $\nu_3/\nu_3+\nu_4-\nu_4$ ratio is the non-auroral 3-μm CH_4 emission on the disk of Jupiter excited by sunlight (Kim et al., 2014). This ratio is also very similar on the disks of Saturn (Kim and Geballe, 2005) and Titan (Kim et al., 2000), because they receive the same intensity ratio of solar radiation at 3.3 and 2.3 μm as Jupiter, although the absolute solar insolations are different.

4. Results and discussion

The nearly constant intensity ratios in Fig. 3 suggest that the polar CH_4 molecules are excited by source(s) whose energy distributions are similar throughout the auroral regions so that the ratios of energy inputs at 3.3 μm and 2.3 μm are similar, although the absolute energy inputs may be different from region to region. The candidates for providing this kind of broad energy sources in the near-IR range are thought to be auroral particle precipitation and/or Joule heating, which should mainly occur above the 1-μbar pressure level, where the atmosphere becomes ionized and the CH_4 mixing ratio rapidly decreases. This is in contrast to the 8-μm CH_4 thermal radiation which forms around the 10–20 μbar level (Drossart et al., 1993), where the CH_4 column density is much higher.

The first step in determining the cause of the different morphologies of the 3- and 8-μm CH_4 bright spots should be an investigation of the radiative processes at the different altitudes where the 3- and 8-μm CH_4 line emission as well as H_3^+ line emission (Lystrup et al., 2008) occur. At present, however, due to lack of vertically resolved observational data over the polar regions, it is premature to investigate the detailed radiative processes in order to determine which of the above candidates is the dominant energy source causing the infrared emission. One of the principal objectives of the Juno Mission is to study Jupiter's magnetosphere near the poles with JIRAM (Jupiter InfraRed Auroral Mapper, Adriani et al., 2008), an on-board IR imager and low-resolution IR spectrometer. Successful observations of vertically resolved auroral CH_4 emission by JIRAM/Juno, which is expected to be at Jupiter in 2016, *may* shed light on these unresolved issues. Interpretation of the Juno observations could be aided by observations of jovian auroral line emission, using ground-based 3- and 8-μm imaging or spectroscopy, which are contemporaneous with Juno's JIRAM and UVS measurements.

Acknowledgments

This paper is based on observations obtained at the Gemini Observatory, which is operated by the Association of Universities for Research in Astronomy, Inc., under a cooperative agreement with the NSF on behalf of the Gemini partnership: the National Science Foundation (United States), the National Research Council (Canada), CONICYT (Chile), the Australian Research Council (Australia), Ministério da Ciência, Tecnologia e Inovação (Brazil) and Ministerio de Ciencia, Tecnología e Innovación Productiva (Argentina). SJK acknowledges support from the Brain Korea 21 Plus (BK21+) program through the National Research Foundation of Korea funded by the Ministry of Education, Science and Technology, and from the Korean Astronomy & Space Science Institute under the R&D program supervised by the Ministry of Science, ICT and Future Planning.

References

Adriani, A. et al., 2008. JIRAM, the image spectrometer in the near infrared on board the Juno mission to Jupiter. Astrobiology 8, 613–622.
Caldwell, J., Tokunaga, A.T., Orton, G.S., 1983. Further observations of 8-μm polar brightenings of Jupiter. Icarus 53, 133–140.
Caldwell, J. et al., 1988. Infrared polar brightenings on Jupiter IV. Spatial properties of methane emission. Icarus 74, 331–339.
Drossart, P. et al., 1993. Thermal profiles in the auroral regions of Jupiter. J. Geophys. Res. 98, 18803–18811.
Drossart, P. et al., 1999. Fluorescence in the 3 micron bands of methane on Jupiter and Saturn from ISO/SWS observations. ESA SP-427, pp. 169–172.
Grodent, D. et al., 2003. Jupiter's main auroral oval observed with HST-STIS. J. Geophys. Res. 106. http://dx.doi.org/10.1029/2003JA009921.
Kim, S.J., Geballe, T.R., 2005. The 2.9–4.2 micron spectrum of Saturn: Clouds and CH_4, PH_3, and NH_3. Icarus 179, 449–458. http://dx.doi.org/10.1016/j.icarus.2009.03.020.
Kim, S.J. et al., 1985. Infrared polar brightening on Jupiter. III. Spectrometry from the Voyager 1 IRIS experiment. Icarus 64, 233–248.
Kim, S.J. et al., 1991. Images of aurorae on Jupiter from H_3^+ emission at 4 μm. Nature 353, 536–539.
Kim, S.J., Geballe, T.R., Noll, K.S., 2000. Three-micrometer CH_4 line emission from Titan's high altitude atmosphere. Icarus 147, 588–591. http://dx.doi.org/10.1006/icar.2000.6481.
Kim, S.J. et al., 2009. Jupiter's hydrocarbon polar brightening: Discovery of 3-micron line emission from south polar CH_4, C_2H_2, and C_2H_6. Icarus 202, 354–357. http://dx.doi.org/10.1016/j.icarus.2009.03.020.
Kim, S.J. et al., 2010. High-resolution 3-μm spectra of Jupiter: Latitudinal spectral variations influenced by molecules, clouds, and haze. Icarus 208, 837–849. http://dx.doi.org/10.1016/j.icarus.2010.03.024.
Kim, S.J. et al., 2014. CH_4 mixing ratios at microbar pressure levels of Jupiter as constrained by 3-micron ISO data. Icarus 237, 42–51. http://dx.doi.org/10.1016/j.icarus.2014.04.023.
Lystrup, M.B. et al., 2008. First vertical ion density profile in Jupiter's auroral atmosphere: Direct observations using the Keck II telescope. Astrophys. J. 677, 790–797.
Rothman, L.S. et al., 2009. The HITRAN 2008 molecular spectroscopic database. J. Quant. Spectrosc. Radiat. Trans. 110, 533–572. http://dx.doi.org/10.1016/j.jqsrt.2009.02.013.
Sada, P.V. et al., 2003. Transient IR phenomena observed by Cassini/CIRS in Jupiter's auroral regions. Bull. Am. Astron. Soc. 35, 402.
Satoh, T., Connerney, J.E.P., Baron, R.L., 1996. Emission source model of Jupiter's H_3^+ Aurorae: A generalized inverse analysis of images. Icarus 122, 1–23.
Wong, A.-S., Lee, A.Y.T., Yung, Y.L., 2000. Jupiter: Aerosol chemistry in the polar atmosphere. Astrophys. J. 534, L215–L217.
Wong, A.-S., Yung, Y.L., Friedson, A.J., 2003. Benzene and haze formation in the polar atmosphere of Jupiter. Geophys. Res. Lett. 30. http://dx.doi.org/10.1029/2002GL016661.